Astrodynamics Vol. 7, No. 2, 251–258, 2023 https://doi.org/10.1007/s42064-022-0150-4

Application of homotopy perturbation method to the radial thrust problem

Lorenzo Niccolai (✉), Alessandro A. Quarta, and Giovanni Mengali

Department of Civil and Industrial Engineering, University of Pisa, I-56122, Italy

ABSTRACT

The dynamics of a spacecraft propelled by a continuous radial thrust resembles that of a nonlinear oscillator. This is analyzed in this work with a novel method that combines the definition of a suitable homotopy with a classical perturbation approach, in which the low thrust is assumed to be a perturbation of the nominal Keplerian motion. The homotopy perturbation method provides the analytical (approximate) solution of the dynamical equations in polar form to estimate the corresponding spacecraft propelled trajectory with a short computational time. The accuracy of the analytical results was tested in an orbital-targeting mission scenario.

KEYWORDS

radial thrust
homotopy perturbation method
nonlinear oscillator
trajectory approximation

Engineering Note

Received: 24 May 2022
Accepted: 4 August 2022

1 Introduction

The study of spacecraft motion under radial propulsive acceleration is a classical problem in spaceflight mechanics, and represents one of the few cases in which some properties of the propelled trajectory can be obtained in an analytical form [1, 2]. Several techniques are available to analyze this problem. For example, Prussing and Coverstone-Carroll [3] proposed a graphical approach to identify the allowable regions of motion when the acceleration magnitude has a constant value. Their results were later extended to the case of variable spacecraft mass [4], and completed by including the J_2 effect in a planetocentric mission scenario [5]. Other approaches use elliptic integrals [6, 7] to describe the spacecraft propelled trajectory. Izzo and Biscani [8] discussed an analytical solution of the spacecraft equations of motion using Weierstrass integrals. More recently, the classical radial thrust problem was analyzed for spacecraft equipped with propellant-less propulsion systems [9], such as solar sails [10–13], electric sails [14, 15], and magnetic sails [16].

In the context of a radial low-thrust mission scenario, that is, when the propulsive acceleration may be considered as a small disturbance of the Keplerian motion, perturbation methods represent a convenient analysis tool [17, 18]. In fact, perturbations based on asymptotic series expansions have recently been used to obtain accurate approximations of spacecraft dynamics in a number of special cases, which differ in terms of the type of propulsion system used by the spacecraft [19, 20] or the thrust vector direction [21, 22].

A well-known technique originally proposed by He [23, 24] combines the typical perturbative approach with a suitably defined homotopy [25, 26]. Although this homotopy perturbation method has been applied to a wide range of science engineering problems [27–31], it has never been applied to approximate the trajectory of a radially accelerated spacecraft. Accordingly, the aim of this work is to present the first application of He's homotopy perturbation method to spacecraft propelled trajectory analysis within the context of the (continuous) radial low-thrust problem. In particular, we discuss the effectiveness of this technique in obtaining an analytical approximation of the spacecraft propelled trajectory when the propulsive acceleration is in the radial direction and has a small and constant magnitude.

The remainder of this paper is organized as follows. After a brief description of the mathematical equations that model the system dynamics, we discuss the application of the homotopy perturbation method and derive an analytical approximation of the spacecraft propelled trajectory. Then, a comparison is made with

✉ lorenzo.niccolai@ing.unipi.it

Nomenclature

$\{a_1, a_2, a_3, a_4\}$	dimensionless coefficients	ρ	dimensionless radial coordinate
a_R	propulsive acceleration magnitude (mm/s^2)	ρ_i	i-th coefficient of power series
		$\overline{\rho}$	linear approximation of ρ
E	dimensionless error	τ	auxiliary parameter
$\mathcal{H}$	homotopy		
k	embedding parameter	*Subscripts*	
$\mathcal{L}$	linear operator	app	analytical approximation
$\mathcal{N}$	nonlinear operator	0	initial parking orbit
r	radial coordinate (km)	f	final
t	time (s)	num	evaluated through orbital propagator
ϵ	dimensionless propulsive acceleration		
θ	polar angle (deg)	*Superscript*	
μ	gravitational parameter (km^3/s^2)	$'$	derivative w.r.t. θ

other existing approximate solutions. Finally, a potential mission application is discussed.

2 Spacecraft propelled trajectory approximation

Consider a spacecraft that initially covers a circular Keplerian orbit with a radius r_0 around a primary body with a gravitational parameter μ. The spacecraft is equipped with a primary propulsion system that provides the radial propulsive acceleration with a small and constant magnitude $a_R \ll \mu/r_0^2$. The thrust vector acts on the plane of the parking orbit for $t \geqslant t_0 \triangleq 0$; hence, the two-dimensional spacecraft trajectory is described by the variation of the radial distance r with the polar angle θ, which is the angle measured counterclockwise from the initial Sun–spacecraft line to the spacecraft position vector direction (see Fig. 1).

Using the polar angle as an independent variable, and paralleling the procedure detailed in Refs. [32, 33], the spacecraft dynamics can be described by the second-order nonlinear differential equation in Eq. (1):

$$\rho'' + \rho - \frac{\tau\epsilon}{(1-\rho)^2} = 0 \tag{1}$$

where the prime symbol denotes the derivative taken with respect to θ, $\tau \in \{-1, 1\}$ is the dimensionless parameter that models either an outward ($\tau = 1$) or inward ($\tau = -1$) propulsive acceleration, and ϵ is the dimensionless value of a_R given by

$$\epsilon \triangleq \frac{a_R}{\mu/r_0^2} \tag{2}$$

ρ is a type of dimensionless radial distance defined as

$$\rho \triangleq 1 - \frac{r_0}{r} \tag{3}$$

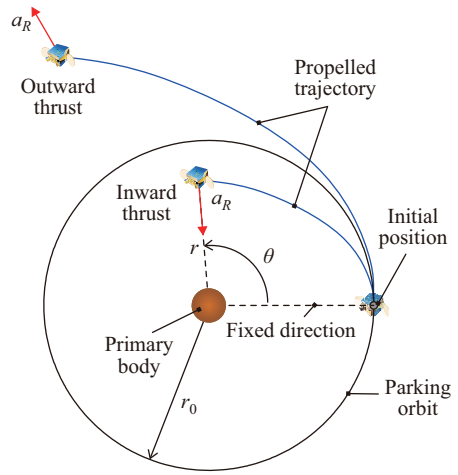

Fig. 1 Sketch of the problem with inward and outward radial thrust.

The differential equation (1) is completed by the initial conditions that model the state of the spacecraft along the circular parking orbit.

$$\rho(0) = 0, \quad \rho'(0) = 0 \tag{4}$$

Note that Eq. (1) describes the dynamics of an equivalent nonlinear oscillator. The application of this equation in the context of trajectory analysis is discussed in Ref. [32] (or Ref. [33]) for the outward (or inward) thrust case. Although the general analytical solution of Eq. (1) exists, it is not given in terms of the elementary functions [6, 8]. To deal with this issue, analytical approximations may be obtained using perturbation methods, that is, by modeling the thrust as a perturbation [34, 35] of the Keplerian motion, as discussed in Section 2.1.

2.1 Homotopy perturbation method

The analysis of the system dynamics described by Eq. (1) is considered with the homotopy perturbation method proposed by He [23]. To this end, the equivalent oscillator dynamics is first decomposed into linear ($\mathcal{L}$) and nonlinear ($\mathcal{N}$) parts:

$$\mathcal{L}(\rho) \triangleq \rho'' + \rho, \quad \mathcal{N}(\rho) \triangleq -\frac{\tau\epsilon}{(1-\rho)^2} \tag{5}$$

such that Eq. (1) can be rewritten as

$$\mathcal{L}(\rho) + \mathcal{N}(\rho) = 0 \tag{6}$$

Then, analogous to Ref. [23], a homotopy $\mathcal{H}(\rho, k)$ is constructed as

$$\mathcal{H}(\rho, k) \triangleq k\left(\mathcal{L}(\rho) + \mathcal{N}(\rho)\right) + (1-k)\left(\mathcal{L}(\rho) - \mathcal{L}(\overline{\rho})\right) \tag{7}$$

where $k \in [0, 1]$ is an embedding dimensionless parameter and $\overline{\rho}$ is a generic linear approximation of the solution of Eq. (1) that satisfies the two initial conditions given by Eq. (4). The motivation behind the introduction of $\mathcal{H}$ becomes clear by writing the auxiliary equation $\mathcal{H}(\rho, k) = 0$, which is simplified as

$$\mathcal{L}(\rho) - \mathcal{L}(\overline{\rho}) + k\left(\mathcal{L}(\overline{\rho}) + \mathcal{N}(\rho)\right) = 0 \tag{8}$$

Indeed, the roots of Eq. (8), which are functions of k, can be changed by simply varying the embedding parameter k within the interval $[0, 1]$. In particular, when $k = 0$, Eq. (8) is reduced to the linear equation $\mathcal{L}(\rho) - \mathcal{L}(\overline{\rho}) = 0$. However, if $k = 1$, Eq. (8) is simplified to $\mathcal{L}(\rho) + \mathcal{N}(\rho) = 0$, which coincides with the actual system dynamics expressed by Eq. (6). In other words, the solution of Eq. (8) varies with k and approaches the solution of the original nonlinear oscillator described by Eq. (6) in the limit as $k \to 1$.

According to Ref. [23], the state variable ρ in Eq. (8) can be expanded in a power series of the embedding parameter k as

$$\rho = \rho_0 + k\rho_1 + k^2\rho_2 + k^3\rho_3 + k^4\rho_4 + \mathcal{O}(k^5) \tag{9}$$

where the coefficients ρ_i are functions of the polar angle θ with zero initial conditions for $i \geqslant 1$.

$$\rho_i(0) = 0, \quad \rho_i'(0) = 0 \quad \text{for} \quad i \geqslant 1 \tag{10}$$

while ρ_0 satisfies the initial conditions of ρ in Eq. (4):

$$\rho_0(0) = 0, \quad \rho_0'(0) = 0 \tag{11}$$

Substituting Eq. (9) into Eq. (8) and equating the zeroth-order terms in k yields

$$\rho_0'' + \rho_0 = \overline{\rho}'' + \overline{\rho} \tag{12}$$

such that $\overline{\rho} \equiv \rho_0$. Without the loss of generality [23], a potential straightforward solution of Eq. (12) that satisfies the initial conditions (11) is selected.

$$\rho_0 = \overline{\rho} \equiv 0 \tag{13}$$

To obtain differential equations describing the dynamics of higher-order terms in k, the nonlinear operator $\mathcal{N}(\rho)$ is approximated with a binomial expansion, assuming that the linear and higher-order terms in k of Eq. (9) have a small magnitude.

$$\begin{aligned}\mathcal{N}(\rho) &= -\frac{\tau\epsilon}{(1-\rho)^2} \\ &= -\frac{\tau\epsilon}{\left(1 - k\rho_1 - k^2\rho_2 - k^3\rho_3 - k^4\rho_4 - \mathcal{O}(k^5)\right)^2} \\ &\simeq -\tau\epsilon\left(1 + 2k\rho_1 + 2k^2\rho_2 + 2k^3\rho_3 + 2k^4\rho_4 + \mathcal{O}(k^5)\right)\end{aligned} \tag{14}$$

in which Eq. (13) has been enforced. Substituting Eqs. (9) and (14) into Eq. (8), the differential equation of the first-order term in k is

$$\rho_1'' + \rho_1 = \tau\epsilon \tag{15}$$

Integrating Eq. (15) with zero initial conditions, as in Eq. (10), yields

$$\rho_1 = \tau\epsilon(1 - \cos\theta) \tag{16}$$

Similarly, the dynamical equation of the second-order term in k is

$$\rho_2'' + \rho_2 = 2\tau\epsilon\rho_1 = 2\epsilon^2(1 - \cos\theta) \tag{17}$$

where Eq. (16) has been used to obtain the last term. Integrating Eq. (17) with zero initial conditions yields

$$\rho_2 = 2\epsilon^2(1 - \cos\theta) - \epsilon^2\theta\sin\theta \tag{18}$$

The same procedure may be applied to the third-order term in k, that is

$$\rho_3'' + \rho_3 = 2\tau\epsilon\rho_2 = 4\tau\epsilon^3(1 - \cos\theta) - 2\tau\epsilon^3\theta\sin\theta \tag{19}$$

whose integral is

$$\rho_3 = 4\tau\epsilon^3(1 - \cos\theta) + \frac{1}{2}\tau\epsilon^3\theta^2\cos\theta - \frac{5}{2}\tau\epsilon^3\theta\sin\theta \tag{20}$$

and to the fourth-order term

$$\rho_4'' + \rho_4 = 2\tau\epsilon\rho_3 = 8\epsilon^4(1 - \cos\theta) + \epsilon^4\theta^2\cos\theta - 5\epsilon^4\theta\sin\theta \tag{21}$$

from which

$$\begin{aligned}\rho_4 = 8\epsilon^4(1 - \cos\theta) &- \frac{11}{2}\epsilon^4\theta\sin\theta \\ &+ \frac{3}{2}\epsilon^4\theta^2\cos\theta + \frac{1}{6}\epsilon^4\theta^3\sin\theta\end{aligned} \tag{22}$$

Note that the coefficients ρ_i (with $i \geqslant 1$) are all proportional to ϵ^i such that the binomial

approximation (14) and corresponding results are valid as long as ϵ (and the propulsive acceleration magnitude a_R) is sufficiently small (see Eq. (2)). It should be noted that the approximation could, in principle, be extended to higher-order terms; however, the increase in accuracy would be negligible compared with the numerical error introduced by the binomial expansion of Eq. (14). Therefore, the approximation is truncated at the fourth order.

Accordingly, a fourth-order approximation of the function $\rho = \rho(\theta)$ can be obtained from Eq. (9) by enforcing the conditions $\mathcal{O}(k^5) = 0$ and $k = 1$, that is,

$$\rho \simeq \rho_0 + \rho_1 + \rho_2 + \rho_3 + \rho_4 \tag{23}$$

Bearing in mind Eqs. (13), (16), (18), (20), and (22), Eq. (23) yields

$$\rho \simeq a_1\,\epsilon + a_2\,\epsilon^2 + a_3\,\epsilon^3 + a_4\,\epsilon^4 \tag{24}$$

where

$$a_1 \triangleq \tau(1-\cos\theta) \tag{25}$$

$$a_2 \triangleq 2(1-\cos\theta) - \theta\sin\theta \tag{26}$$

$$a_3 \triangleq 4\tau(1-\cos\theta) - \frac{5}{2}\tau\theta\sin\theta + \frac{1}{2}\tau\theta^2\cos\theta \tag{27}$$

$$a_4 \triangleq 8(1-\cos\theta) - \frac{11}{2}\theta\sin\theta + \frac{3}{2}\theta^2\cos\theta + \frac{1}{6}\theta^3\sin\theta \tag{28}$$

Finally, the polar form of the spacecraft propelled trajectory is retrieved from Eq. (3) as Eq. (29):

$$r(\theta) = \frac{r_0}{1-\rho(\theta)} \simeq \frac{r_0}{1 - a_1\,\epsilon - a_2\,\epsilon^2 - a_3\,\epsilon^3 - a_4\,\epsilon^4} \tag{29}$$

2.2 Model validation

The accuracy of the trajectory approximated by Eqs. (24)–(29) is tested by taking the outputs of an orbital propagator as reference values, in which Eq. (1) was integrated in double precision using a variable order Adams–Bashforth–Moulton solver scheme [36, 37] with absolute and relative errors of 10^{-12}. The performance of the proposed technique is compared with that of a second-order perturbation method based on an asymptotic series expansion, the results of which were applied in Ref. [33] to approximate the spacecraft trajectory in the case of inward (radial) propulsive acceleration, but may also be generalized to include the outward case as

$$r(\theta) = \frac{r_0}{1 - \tau\epsilon(1-\cos\theta) + \epsilon^2(2\cos\theta - 2 + \theta\sin\theta)} \tag{30}$$

The latter expression slightly differs from that reported in Ref. [33] where $\tau = -1$. This is because in this work, the polar angle θ was measured from the primary body-spacecraft line at time t_0 (see Fig. 1). Note that the outputs of the orbital propagator were chosen as reference values instead of the results obtained with the analytical method based on elliptic integrals discussed in Ref. [6] because of the reduced computational time required by the orbital propagator. However, some tests have been performed to compare the results of the approximation method with those obtained by the analytical solution. The results are practically identical to those discussed in the remainder of this section.

To compare the performance of the two approximation methods, a dimensionless error is defined as

$$E \triangleq \left| \frac{r_{\mathrm{app}} - r_{\mathrm{num}}}{r_{\mathrm{num}}} \right| \tag{31}$$

where r_{app} is the radial distance at a generic polar angle θ estimated with Eq. (29) or Eq. (30), and r_{num} is the actual radial coordinate calculated with the (numerical) orbital propagator. The variations in dimensionless errors E obtained with Eqs. (29) and (30) when $\epsilon = 1\%$ are shown in Figs. 2(a) and 2(b) for an outward thrust ($\tau = 1$) and inward thrust ($\tau = -1$), respectively. Although the accuracy of both approximations decreased as the polar angle θ increased, it is clear from Fig. 2 that the homotopy perturbation method significantly outperformed the asymptotic series technique used in Ref. [33].

The accuracy of the analytical approximation (29)

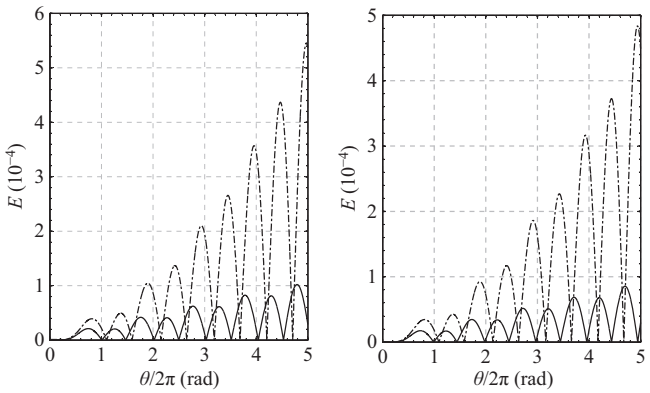

(a) Outward thrust ($\tau = 1$) (b) Inward thrust ($\tau = -1$)

Fig. 2 Comparison between the accuracy of the asymptotic series method of Ref. [33] (dash-dot line) and the homotopy perturbation approach (continuous line) as functions of θ when $\epsilon = 1\%$.

decreased as the dimensionless propulsive acceleration magnitude ϵ increased. This is because the binomial expansion of Eq. (14) is valid as long as ρ is small, that is, as long as $\epsilon \ll 1$ (see Eq. (24)). However, if the variation of the polar angle is sufficiently small, Eq. (29) provides an accurate approximation of the actual radial distance even when ϵ reaches a few tenths. For example, if $\theta \leqslant 90$ deg, then the maximum value of E varied with $\epsilon \in (0, 0.25]$, as shown in Fig. 3. In the worst case, when $\epsilon = 0.25$ and $\tau = 1$, Fig. 3(a) shows that Eq. (29) approximates the actual radial distance with a dimensionless error of less than 1%. If $\epsilon < 0.05$, then the error decreased to $\max(E) < 5 \times 10^{-5}$. Note that the combination of $\epsilon = 0.25$ and $\tau = 1$ allows the spacecraft to reach the maximum radial distance of approximately $1.4r_0$ when $\theta \in [0, 90]$ deg, as shown in Fig. 4(a). Figure 4(b) shows the variation in the minimum r as a function of ϵ when

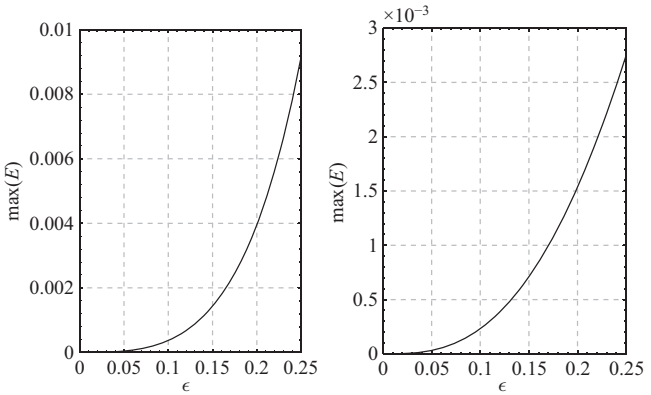

(a) Outward thrust ($\tau = 1$) (b) Inward thrust ($\tau = -1$)

Fig. 3 Maximum value of E as a function of ϵ when $\theta \leqslant 90$ deg.

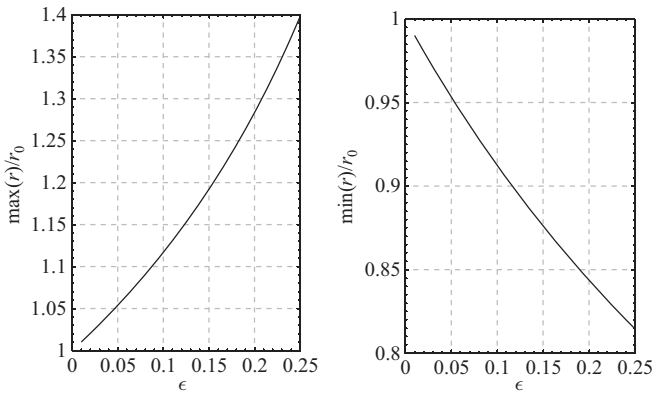

(a) Outward thrust ($\tau = 1$) (b) Inward thrust ($\tau = -1$)

Fig. 4 Maximum or minimum value of the radial distance as a function of ϵ when $\theta \leqslant 90$ deg.

$\tau = -1$. In this case, when $\epsilon = 0.25$ and $\tau = -1$, a minimum primary-spacecraft distance slightly smaller than $0.82r_0$ was obtained for the same polar angle value.

The approximate solution reduced the computational time by approximately two orders of magnitude compared with that required by an orbital propagator. However, the solution discussed in Ref. [6], despite being analytical, is only capable of providing the swept angle θ as a function of r because it requires the solution of an elliptic integral for each pair $\{r_0, r\}$ to obtain the corresponding value of θ. In other words, although the results reported in Ref. [6] are useful for calculating the flight time and swept angle between two positions, the solution discussed in this work can approximate the polar form of the spacecraft propelled trajectory much more quickly.

3 Potential mission application

The analytical approximation of Eq. (24) (or of Eq. (29)) can be used to quickly solve a type of targeting problem, the aim of which is to select the propulsive acceleration magnitude required by a radially accelerated spacecraft to reach the target point of given polar coordinates $\{r_\mathrm{f}, \theta_\mathrm{f}\}$.

For example, assume that $\theta_\mathrm{f} = 90$ deg and $r_\mathrm{f} = 1.2r_0$ such that the target dimensionless radial distance is $\rho_\mathrm{f} = 1 - r_0/r_\mathrm{f} \simeq 0.166$. In this case, considering an outward radial thrust ($\tau = 1$) and using Eq. (24), the condition $\rho = \rho_\mathrm{f}$ yields the fourth-order polynomial equation:

$$(6.5843 \times 10^{-3})\epsilon^4 + (7.3009 \times 10^{-2})\epsilon^3 + 0.4292\,\epsilon^2 + \epsilon - 0.166 = 0 \tag{32}$$

which provides the propulsive acceleration magnitude of $\epsilon \simeq 0.15595$; this value is consistent with Fig. 4(a). The propelled trajectory obtained with the analytical approximation is shown in Fig. 5. It can be seen that it practically coincides with that estimated by the orbital propagator. Note that similar results can be obtained with the second-order approximation of ρ, that is, by assuming $a_3 = a_4 \equiv 0$ in Eq. (24). In this case, the simulations showed that the target point was reached with a dimensionless error of $E \simeq 1.63 \times 10^{-3}$, a value consistent with Fig. 3(a).

4 Conclusions

This paper discussed the application of the homotopy perturbation method in the trajectory analysis of a spacecraft propelled by radial acceleration of a small

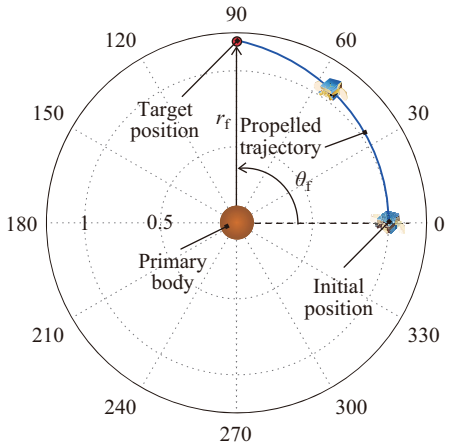

Fig. 5 Propelled trajectory estimated by the analytical approximation for $r_f = 1.2r_0$ and $\theta_f = 90$ deg.

and constant magnitude. The spacecraft dynamics is equivalent to that of a nonlinear oscillator, whose approximate solution was derived by defining a suitable homotopy and modeling the thrust as a perturbative term in Keplerian motion. The accuracy of the obtained polar equation was validated by comparison with the output of an orbital propagator.

The simulation results showed small errors in the trajectory approximation, and confirmed that the homotopy perturbation method significantly outperforms the previously proposed approximate solution. In particular, the analytical approximation of the spacecraft trajectory can be used to analyze a simplified targeting scenario without numerical simulations. The computational time required by the proposed approximation is significantly shorter than that of an orbital propagator or existing analytical solutions based on elliptic integrals.

Funding note

Open Access funding provided by Università di Pisa within the CRUI-CARE Agreement.

Declaration of competing interest

The authors have no competing interests to declare that are relevant to the contents of this article.

References

[1] Tsien, H. S. Take-off from satellite orbit. *Journal of the American Rocket Society*, **1953**, 23(4): 233–236.

[2] Battin, R. H. *An Introduction to the Mathematics and Methods of Astrodynamics*. American Institute of Aeronautics and Astronautics, Inc., **1999**: 408–418.

[3] Prussing, J. E., Coverstone-Carroll, V. Constant radial thrust acceleration redux. *Journal of Guidance, Control, and Dynamics*, **1998**, 21(3): 516–518.

[4] Quarta, A. A., Mengali, G. Radially accelerated trajectories for variable mass spacecraft. *Aerospace Science and Technology*, **2015**, 43: 219–225.

[5] Urrutxua, H., Lara, M. Constant, radial low-thrust problem including first-order effects of J2. *Journal of Guidance, Control, and Dynamics*, **2016**, 39(12): 2766–2771.

[6] Akella, M. R. On low radial thrust spacecraft motion. In: Proceedings of the Astrodynamics Symposium, College Station (TX), USA, **2000**.

[7] Urrutxua, H., Morante, D., Sanjurjo-Rivo, M., Peláez, J. DROMO formulation for planar motions: Solution to the Tsien problem. *Celestial Mechanics and Dynamical Astronomy*, **2015**, 122(2): 143–168.

[8] Izzo, D., Biscani, F. Explicit solution to the constant radial acceleration problem. *Journal of Guidance, Control, and Dynamics*, **2014**, 38(4): 733–739.

[9] Bassetto, M., Quarta, A. A., Mengali, G., Cipolla, V. Spiral trajectories induced by radial thrust with applications to generalized sails. *Astrodynamics*, **2021**, 5(2): 121–137.

[10] Gong, S., Macdonald, M. Review on solar sail technology. *Astrodynamics*, **2019**, 3(2): 93–125.

[11] Quarta, A. A., Mengali, G., Niccolai, L. Smart dust option for geomagnetic tail exploration. *Astrodynamics*, **2019**, 3(3): 217–230.

[12] Vulpetti, G., Circi, C., Pino, T. Coronal Mass Ejection early-warning mission by solar-photon sailcraft. *Acta Astronautica*, **2017**, 140: 113–125.

[13] Bassetto, M., Niccolai, L., Boni, L., Mengali, G., Quarta, A. A., Circi, C., Pizzurro, S., Pizzarelli, M., Pellegrini, R. C., Cavallini, E. Sliding mode control for attitude maneuvers of Helianthus solar sail. *Acta Astronautica*, **2022**, 198: 100–110.

[14] Mengali, G., Quarta, A. A., Aliasi, G. A graphical approach to electric sail mission design with radial thrust. *Acta Astronautica*, **2013**, 82(2): 197–208.

[15] Bassetto, M., Niccolai, L., Quarta, A. A., Mengali, G. A comprehensive review of Electric Solar Wind Sail concept and its applications. *Progress in Aerospace Sciences*, **2022**, 128: 100768.

[16] Bassetto, M., Quarta, A. A., Mengali, G. Generalized sail trajectory approximation with applications to MagSails. *Aerospace Science and Technology*, **2021**, 118: 106991.

[17] Peláez, J., Hedo, J. M., Andrés, P. R. A special

perturbation method in orbital dynamics. *Celestial Mechanics and Dynamical Astronomy*, **2007**, 97(2): 131–150.

[18] Avanzini, G., Palmas, A., Vellutini, E. Solution of low-thrust lambert problem with perturbative expansions of equinoctial elements. *Journal of Guidance, Control, and Dynamics*, **2015**, 38(9): 1585–1601.

[19] Niccolai, L., Quarta, A. A., Mengali, G. Solar sail trajectory analysis with asymptotic expansion method. *Aerospace Science and Technology*, **2017**, 68: 431–440.

[20] Niccolai, L., Quarta, A. A., Mengali, G. Two-dimensional heliocentric dynamics approximation of an electric sail with fixed attitude. *Aerospace Science and Technology*, **2017**, 71: 441–446.

[21] Bombardelli, C., Baù, G., Peláez, J. Asymptotic solution for the two-body problem with constant tangential thrust acceleration. *Celestial Mechanics and Dynamical Astronomy*, **2011**, 110(3): 239–256.

[22] Niccolai, L., Quarta, A. A., Mengali, G. Orbital motion approximation with constant circumferential acceleration. *Journal of Guidance, Control, and Dynamics*, **2018**, 41(8): 1783–1789.

[23] He, J. H. Homotopy perturbation technique. *Computer Methods in Applied Mechanics and Engineering*, **1999**, 178(3–4): 257–262.

[24] He, J. H. Homotopy perturbation method with an auxiliary term. *Abstract and Applied Analysis*, **2012**, 2012: 857612.

[25] Liao, S. J. An approximate solution technique not depending on small parameters: A special example. *International Journal of Non-Linear Mechanics*, **1995**, 30(3): 371–380.

[26] Liao, S. J. Boundary element method for general nonlinear differential operators. *Engineering Analysis with Boundary Elements*, **1997**, 20(2): 91–99.

[27] Sedighi, H., Daneshmand, F. Nonlinear transversely vibrating beams by the homotopy perturbation method with an auxiliary term. *Journal of Applied and Computational Mechanics*, **2014**, 1(1): 1–9.

[28] Sullo, N., Peloni, A., Ceriotti, M. Low-thrust to solar-sail trajectories: A homotopic approach. *Journal of Guidance, Control, and Dynamics*, **2017**, 40(11): 2796–2806.

[29] He, J. H., El-Dib, Y. O. Homotopy perturbation method for Fangzhu oscillator. *Journal of Mathematical Chemistry*, **2020**, 58(10): 2245–2253.

[30] Elías-Zúñiga, A., Palacios-Pineda, L. M., Jiménez-Cedeño, I. H., Martínez-Romero, O., Trejo, D. O. He's frequency–amplitude formulation for nonlinear oscillators using Jacobi elliptic functions. *Journal of Low Frequency Noise, Vibration and Active Control*, **2020**, 39(4): 1216–1223.

[31] Akinyemi, L., Şenol, M., Huseen, S. N. Modified homotopy methods for generalized fractional perturbed Zakharov–Kuznetsov equation in dusty plasma. *Advances in Difference Equations*, **2021**, 2021: 45.

[32] Quarta, A. A., Mengali, G. New look to the constant radial acceleration problem. *Journal of Guidance, Control, and Dynamics*, **2012**, 35(3): 919–929.

[33] Niccolai, L., Quarta, A. A., Mengali, G. Approximate solution of spacecraft motion with an inward constant radial acceleration. *Aerospace Science and Technology*, **2022**, 120: 107288.

[34] Lei, H. L. Dynamical models for secular evolution of navigation satellites. *Astrodynamics*, **2020**, 4(1): 57–73.

[35] He, B. Y., Shen, H. X. Solution set calculation of the Sun-perturbed optimal two-impulse trans-lunar orbits using continuation theory. *Astrodynamics*, **2020**, 4(1): 75–86.

[36] Shampine, L. F., Gordon, M. K. *Computer Solution of Ordinary Differential Equations: The Initial Value Problem*. San Francisco, USA: W. H. Freeman & Co Ltd., **1975**.

[37] Shampine, L. F., Reichelt, M. W. The MATLAB ODE suite. *SIAM Journal on Scientific Computing*, **1997**, 18(1): 1–22.

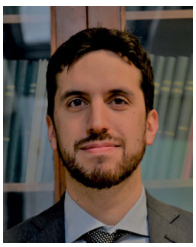

Lorenzo Niccolai received his Ph.D. degree in industrial engineering (aerospace curriculum) from the University of Pisa in 2018. He was a research assistant at the Department of Civil and Industrial Engineering of the University of Pisa from 2019 to 2020. He is currently an assistant professor of spaceflight mechanics at the same department. His research interests include mission design, low-thrust trajectory analysis and control, with special attention on innovative propulsive concepts such as solar sails and electric solar wind sails. E-mail: lorenzo.niccolai@ing.unipi.it.

Alessandro A. Quarta received his Ph.D. degree in aerospace engineering from the University of Pisa in 2005 and, currently, he is a professor of flight mechanics at the Department of Civil and Industrial Engineering of the University of Pisa. His main research areas include spaceflight simulation, spacecraft mission analysis and design, low-thrust trajectory optimization, and solar sail and E-sail dynamics and control. E-mail: a.quarta@ing.unipi.it.

Giovanni Mengali received his Doctor Engineering degree in aeronautical engineering in 1989 from the University of Pisa. Since 1990, he has been with the Department of Aerospace Engineering (now Department of Civil and Industrial Engineering) of the University of Pisa, first as a Ph.D. student, then as an assistant and an associate professor. Currently, he is a professor of space flight mechanics. His main research areas include spacecraft mission analysis, trajectory optimization, and solar sails, electric sails and aircraft flight dynamics and control. E-mail: g.mengali@ing.unipi.it.